

Preliminary Experiments with an Actively Tuned Passive Dynamic Running Robot

M. Ahmadi and M. Buehler

Centre for Intelligent Machines, Department of Mechanical Engineering
McGill University, Montréal, Québec, Canada, H3A 2A7

Abstract: This paper describes experiments with an electrically actuated one legged hopping robot, the ARL Monopod. While a spring-mass system, comprised of the leg spring and the body mass has previously provided the basic “passive dynamic” vertical motion, we have now added a spring in series with the hip actuator to use the same passive dynamic principle for the leg swing motion. This paper validates our previously proposed hip actuation controller, which actively tunes the leg swing motion during running to remain close to its passive dynamic response, and at the same time maintains balance and controls the robot’s desired forward speed. Experimental data of stable running at $1m/s$ show a 75% reduction in hip actuation energy during flight, and a mechanical energy expenditure for the complete robot of only $64W$. The resulting specific resistance of the robot reduces to 0.36 at $1m/s$, which is about half the previously reported result for the robot without hip spring.

1. Introduction

Energy autonomy is a necessity for virtually any practical mobile robot. Achieving the required energy efficient running or walking in legged robots is particularly challenging, since much energy can be expended for internal motions, like vertical body motion, or swinging the legs. Since these motions do not contribute directly to mobility, the energy used to produce them should be minimized.

Just like a pendulum produces periodic motion efficiently by cycling kinetic and gravitational potential energy, the periodic internal motions needed in running can be produced efficiently as well, by cycling kinetic and spring potential energies. Many animals are superbly designed to exploit this principle, and manage to reduce the metabolic cost of running considerably by utilizing the elastic properties of their muscles, tendons, and bones [2].

In the area of robotic systems, it was Raibert [9] who pioneered the use of a system’s unforced response (its “passive dynamics”) to generate the gross motion for locomotion. To date, virtually all dynamically stable running robots utilize an actively tuned spring-mass system to provide the vertical robot motion [9, 8, 4, 6]. A beautiful example of just how far the passive dynamics approach can be carried is provided by McGeer [7] who built a two legged walking

robot with knees, which was able to walk down shallow inclines, driven entirely by gravity without any actuation.

In [5] we show that at $1.2m/s$ the ARL Monopod uses about half of its total energy expenditure for swinging the leg. Much of this energy can be saved, since passive dynamics can provide the leg swing motion via a spring connecting the leg and the body at the hip joint as proposed in [10]. In our previous work [1], we presented a new control strategy to stabilize passive dynamic running of a one-legged robot. An alternative approach for controlling the same robot system with compliant leg and hip was proposed by François and Samson [3]. The controller is derived based on a simplified and linearized dynamic model of the robot, and was shown to be both stable and robust in simulations.

The current paper is devoted to the experimental validation of a controller [1] proposed earlier. In Sec. 2 the robot model and the design modifications to the ARL Monopod are described which give rise to the “ARL Monopod II.” The hip and leg controllers are described in Sec. 3, together with the experimental results. Finally, Sec. 4 computes and discusses the energy expenditure as well as the specific resistance.

2. ARL Monopod II

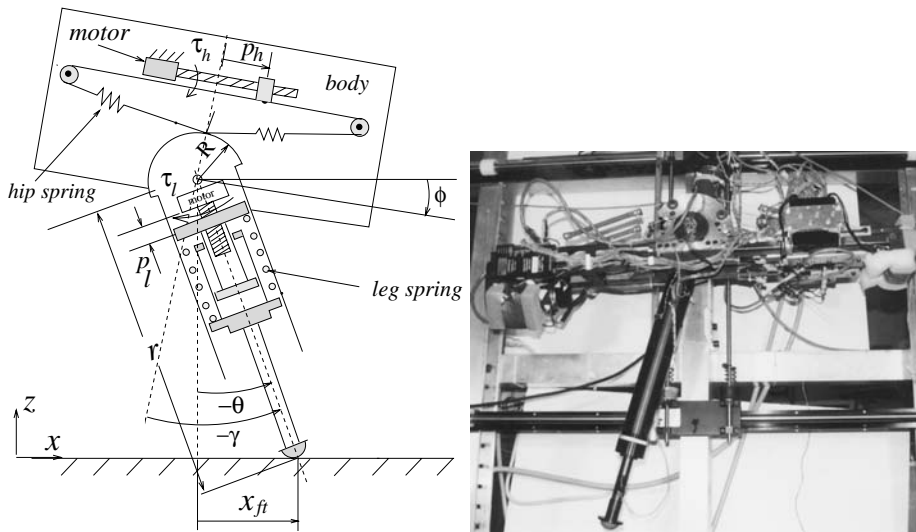


Figure 1. A sketch of ARL Monopod II with important variables, and a photo.

The ARL Monopod II is constrained to move in a vertical plane and consists of a body which is connected to a prismatic leg at the hip joint. A sketch of the mechanical system showing its degrees of freedom, together with a photo is presented in Fig. 1. The system has a total of seven degrees of freedom, including the leg length (r), leg actuator displacement (p_l), hip actuator displacement (p_h), leg angle (θ), and three degrees of freedom of the body (x, z , and body pitch angle ϕ). Due to kinematic constraints, not all of them are free

simultaneously. During stance there are five degrees of freedom $(\theta, \phi, r, p_h, p_l)$, and during flight there are six $(x, z, \theta, \phi, p_h, p_l)$. The nominal values for some of the important parameters are also given in Table 1, followed by a table of indices.

J_b	body inertia	0.8 kgm^2
J_l	leg inertia	$0.12 - 0.19 \text{ kgm}^2$
k_h	hip spring stiffness (linear)	3800 N/m
k_l	leg spring stiffness	6312 N/m
m_b	body mass	11.5 kg
m_l	leg mass	4.6 kg
r_0	leg length (when $p_l = 0$ in flight)	0.64 m

Table 1. *Nomenclature and numerical settings.*

d	desired value	h	hip	f	flight
ll	lower leg	u	upper-leg	cg	center of gravity
$\hat{}$	amplitude	l	leg	lo	lift-off
$*$	passive dynamic	s	stance	td	touchdown
b	body	act	actuator	bu	body+upperleg

Table 2. *Description of indices.*

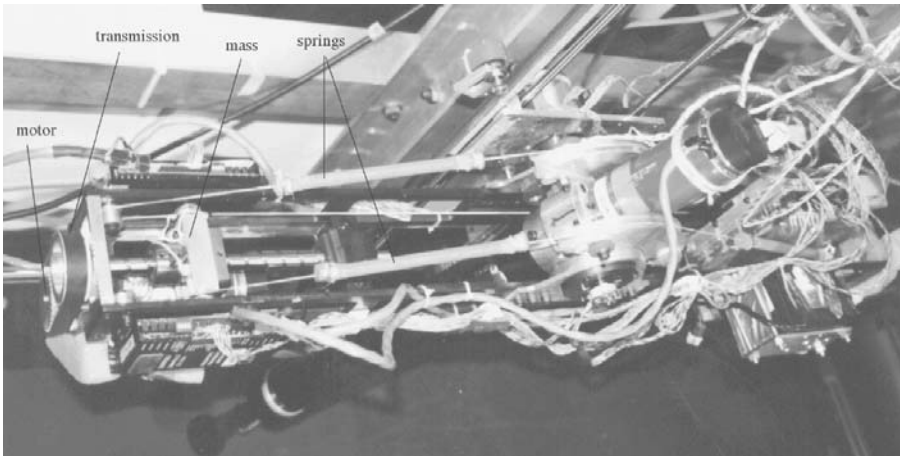


Figure 2. *A closeup of two of the four series hip compliances, inserted in the connecting strings between hip actuation ball screw transmission and leg.*

Both hip and leg actuators are connected in series with springs. The prismatic leg joint features a conventional helical compression spring. The hip has an extension spring made of natural rubber in the form of standard surgical tubing as shown in Fig. 2. Since the hip actuation mechanism employs Spectra strings, which transmit the linear ball screw motion via pulleys to the circular arc attached to the leg, cutting the strings and inserting the tubular spring

offered an effective means of adding hip compliance. With four string locations where the springs could be added in parallel, the energy storage density requirements of the springs were drastically reduced as well. Even though the rubber springs show nonlinear behaviour at low and very large strains, we were able to operate in the linear region by suitable pre-loading, where the stiffness of each individual tubular spring is characterized by $\bar{k}_{latex} = C_{latex}/l_{latex}$. l_{latex} is the length of the spring, and $C_{latex} = 51.5N$ is our springs' particular material constant.

3. Control

The basic control approach builds on Raibert's original idea of controlling hopping height, forward speed, and body pitch via three decoupled controllers [9]. Body pitch and hopping height are controlled during stance, while forward speed is controlled via touchdown foot placement during flight. After modifying Raibert's controller for the control of the passive dynamic hip oscillations, energy consumption was drastically reduced, while stable running was maintained as shown in Fig. 3.

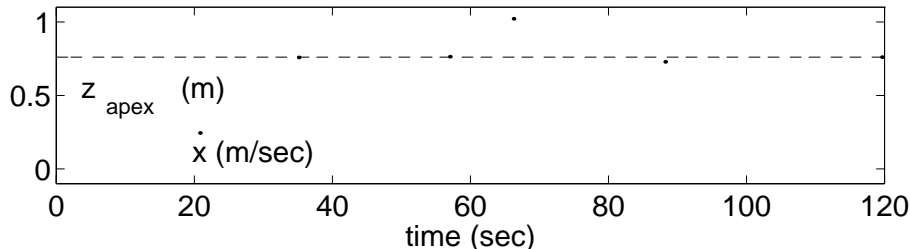


Figure 3. *Experimental data of controlled passive dynamic running. Robot speed \dot{x} and hopping height z_{apex} are recorded during a two minute run. The robot follows a trapezoidal velocity profile from zero to 1m/s. At the same time, the hopping height controller maintains closely the desired apex height.*

3.1. Hopping height control

The performance of the hopping height control is of critical importance to the success of the other controllers which are synchronized to the vertical motion. Any changes in hopping height will act as perturbations to the other controllers. Throughout the experiments, the robot is commanded to maintain a constant (desired) hopping height, $z_{apex,d}$. An energy based controller is used to accomplish this task. Note that the desired hopping height can be translated into a unique desired total vertical energy at apex, $E_{apex}(z_{apex,d})$. The objective of this controller is then to keep the *vertical total energy* of the robot,

$$E_v = E_{pot} + E_{kin,v} \quad (1)$$

at the desired level, where E_{pot} is the gravitational and leg spring potential energy, and $E_{kin,v}$ the vertical component of the kinetic energy. Each step starts at apex and ends at the next apex. Let the vertical energy, E_v , at the

n_{th} apex be E_{apex}^n and let the n_{th} stance be occurring after the n_{th} apex. The difference between the desired energy and actual energy at the n_{th} apex is the amount of energy that we are adding to the system during the subsequent (the n_{th}) stance phase,

$$E_{act,d}^n = E_{apex}^n - E_{apex,d} + \hat{E}_{loss}.$$

\hat{E}_{loss} is an estimate of the energy loss between two successive apexes. As an estimate we use the average of the past two losses,

$$\hat{E}_{loss} = \frac{1}{2}(E_{loss}^{n-1} + E_{loss}^{n-2})$$

where E_{loss}^{n-1} is the measured loss between $(n-1)_{th}$ and the n_{th} apex as,

$$E_{loss}^{n-1} = E_{apex}^{n-1} - E_{apex}^n + E_{act}^{n-1}$$

and E_{act}^{n-1} is the energy added by the leg actuator during the $(n-1)_{th}$ stance. It can be measured directly from the spring force and the actuator's linear velocity at the output of the leg ball screw transmission as

$$E_{act} = \int_{stance} F_l \dot{p}_l dt.$$

The remaining task is to add mechanical energy equal to $E_{act,d}^n$ to the vertical energy of the system during stance. A simple velocity controller can be used to control the injected energy by commanding the desired leg actuator velocity, $\dot{p}_{l,d}$ as a function of the continuously measured energy error,

$$\dot{p}_{l,d} = \kappa_{E1}(E_{act} - E_{act,d}^n).$$

However, this approach completely ignores the actuator dynamics. For example, at the beginning of stance this controller is likely to saturate the leg actuator. In addition, it injects most of the energy right after touchdown when the spring force is small. This results in high ball screw velocities, and as a result, higher damping losses than necessary and also high energy losses for accelerating and decelerating the ball screw. A better strategy is to add this energy when the spring is more compressed and eliminate actuator motion at touchdown and liftoff. To do this we multiply the above expression with a heuristic correction factor

$$\zeta = 1 - \frac{q_l}{q_{l,0}}$$

where q_l is the leg spring length and $q_{l,0}$ is the leg spring rest length. Thus ζ attains its maximum at maximum spring compression and vanishes at touchdown and liftoff.

A velocity feedback controller with feedforward compensation of the leg spring force, F_l , is used to follow the desired velocity,

$$\tau_l = -\kappa_{E2}(\dot{p}_l - \dot{p}_{l,d}) + r_l F_l,$$

where r_l is the leg ball screw lead in m/rad .

Fig. 4 shows experimental running data where the controller successfully injects various desired energy levels. Even when dynamic coupling with the forward motion exists, the controller performs well: Fig. 3 shows how the robot successfully maintains the desired hopping height even while the forward speed varies between zero and $1m/s$.

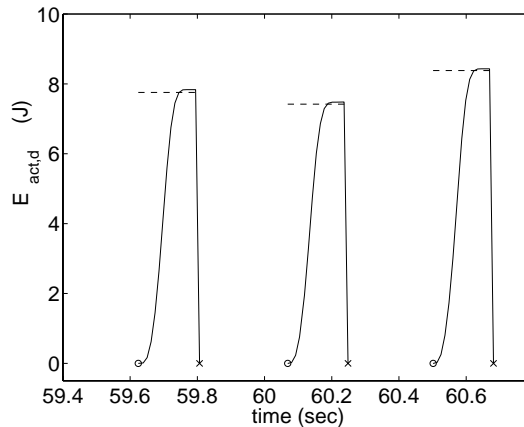


Figure 4. *The performance of the hopping height controller in adding the desired energy (dashed line) during three successive stance phases.*

Since the leg swing motion, described below, must be synchronized to the vertical motion, it is convenient to derive a scalar variable, termed “Locomotion Time,” η , whose amplitude is independent of the hopping height. During flight we use the expression

$$\eta_f = \frac{-\dot{z}}{\dot{z}_{lo}}. \quad (2)$$

If we assume that the robot’s mass is dominated by body mass and follows a ballistic motion during the flight phase, η_f is linear in time, since (2) is equivalent to

$$\eta_f = \frac{2}{T_f}t, \quad (3)$$

and $\eta_f \in [-1, 1]$, $\eta_f(t_{lo}) = -1$, $\eta_f(t_{td}) = 1$. During stance the locomotion time is simply a shifted and scaled time,

$$\eta_s = \frac{2}{T_s}t, \quad \eta_s(t_{td}) = 1, \quad \eta_s(t_{lo}) = -1,$$

where T_s is the previous stance time, used as a prediction of the current stance time. Note that for the definitions of the locomotion times, the time parameter is assumed to be zero at mid-phase.

3.2. Forward speed control

The basic idea behind the use of passive dynamic motion in the hip is illustrated in Fig. 5, and is presented in more detail in [1]. If we denote by x_{ft} the

horizontal position of the toe with respect to the hip, a completely unforced, frictionless counter-oscillation of the leg and body coupled by the hip spring produces a sinusoidal response. It can now be seen that, with proper initial conditions and coordination with the vertical motion, one can assure that stance phase occurs during the period of approximately constant slope, equivalent to the robot forward speed. Thus the unforced response can provide the correct gross hip motion required for locomotion with minimal actuation, and thus energy consumption.

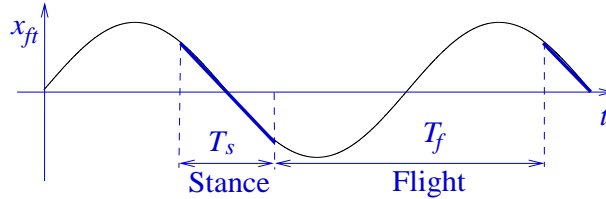


Figure 5. *Foot position with respect to hip, x_{ft} , produced by unforced (passive dynamic) leg swing motion, with linear approximations of stance phase (from [1])*

One complete vertical hopping cycle has to be synchronized with one complete leg swing cycle and where the robot touches ground with the proper leg touchdown angle. During flight, this can be achieved via

$$\theta_d(\eta_f) = \hat{\theta}_d \sin(\pi(1 - \rho)\eta_f), \quad (4)$$

where the duty factor, ρ , is defined as the ratio between stance time and one whole step duration,

$$\rho = \frac{T_s}{T_{step}},$$

and η_f is the flight locomotion time (3). At apex, $\theta_d(\eta_f = 0) = 0$, at liftoff $\theta_d(\eta_f = -1) = -\hat{\theta}_d \sin(\pi(1 - \rho))$ and at touchdown $\theta_d(\eta_f = 1) = \hat{\theta}_d \sin(\pi(1 - \rho))$. The duty factor, determined via the robot's design parameters, is selected such that the frequency of the desired leg angle trajectory (4), when synchronized to the vertical dynamics, can be the unforced response of the dynamical system consisting of the body and the leg, connected via the hip spring. The desired amplitude of the oscillation,

$$\hat{\theta}_d = \frac{\theta_{td,d}}{\sin(\pi(1 - \rho))}$$

is determined by the desired leg touchdown angle, $\theta_{td,d}$, which in turn is determined by the robot's forward speed. Thus the overall leg angle controller, outlined in Fig. 6 determines the desired trajectory from the passive dynamics (4), whose amplitude is determined from the robot's forward speed (via the proper foot placement), and the resulting reference trajectory is then controlled via a model based leg angle controller. A more detailed description of these arguments is provided in [1].

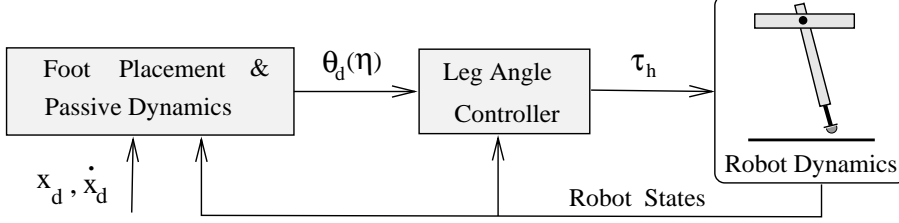


Figure 6. *The general outline of the control for the leg swing angle tracking in the flight phase*

The robot's forward speed is controlled during flight by servoing the leg to the proper touchdown angle. Raibert's foot placement algorithm [9] is used to find the desired foot position at touchdown,

$$x_{ft,td,d} = \frac{1}{2}\dot{x}T_s + \kappa_x(x - x_d) + \kappa_{\dot{x}}(\dot{x} - \dot{x}_d).$$

The first term on the RHS is the neutral foot position with respect to the hip, necessary to maintain the current forward speed. It uses the previous stance time as an estimate of the upcoming stance time. The other two terms are position and velocity error terms necessary for stable tracking. From geometry, the corresponding desired leg touchdown angle is

$$\theta_{td,d} = -\sin^{-1} \frac{x_{f,td,d}}{r}.$$

This completes the derivation of the desired leg angle trajectory derivation.

The tracking controller uses a simplified dynamic model. Assuming that the changes in the actuator position do not have significant dynamic effects except changing the leg inertia,

$$J_l(p_l) = J_{l,min} + (m_{ll} + m_{act})[(p_l + p_{l,0})^2 - p_{l,0}^2].$$

In addition, during the flight we neglect the friction forces acting on the robot through planarizer guides. We consider all the damping forces are small compared to inertial and spring forces. The resulting equations of motion in that case are

$$\begin{aligned} J_b \ddot{\phi} &= Rk_h [p_h + R(\theta - \phi)] \\ J_l \ddot{\theta} &= -Rk_h [p_h + R(\theta - \phi)] \end{aligned} \quad (5)$$

and the coupled actuator dynamics is

$$\alpha_h \ddot{p}_h = \tau_h - rk_h [p_h + R(\theta - \phi)]. \quad (6)$$

The above set of equations results in a system of six coupled first order differential equations. The control problem can be simplified considerably if we assume that the actuator bandwidth is much higher than that of the required leg oscillations. In that case, the control problem can be decoupled into two stages.

Actuator displacement control: The desired actuator displacement commanded by the either the leg angle controller during flight or the body pitch controller during stance is tracked using the model of the actuator dynamics (6). If the desired error dynamics for $e_{ph} = p_{h,d} - p_h$ are

$$\ddot{e}_{ph} + K_{v,f2}\dot{e}_{ph} + K_{p,f2}e_{ph} = 0,$$

the necessary controller is

$$\tau_h = \alpha_h [\ddot{p}_{h,d} + K_{v,f2}\dot{e}_{ph} + K_{p,f2}e_{ph}] + r_h k_h [p_h + R(\theta - \phi)] + r_h c_h [\dot{p}_h + R(\dot{\theta} - \dot{\phi})]. \quad (7)$$

The performance of the controller during a $1m/s$ run is shown in Fig. 7.

Leg Angle Control: Considering the hip actuator displacement p_h as the control input we develop a model based controller for leg angle tracking. The result is the desired hip actuator position which will be used in (7). If the desired final equation for the leg angle error, e_θ is

$$\ddot{e}_\theta + K_{v,f1}\dot{e}_\theta + K_{p,f1}e_\theta = 0,$$

then the input to the system (5), namely the desired hip actuator displacement, $p_{h,d}$ and its corresponding derivatives are

$$\begin{aligned} p_{h,d} &= -R(\theta - \phi) - \frac{J_l}{Rk_h} \left[\ddot{\theta}_d + K_{v,f1}\dot{e}_\theta + K_{p,f1}e_\theta \right], \\ \dot{p}_{h,d} &= -R(\dot{\theta} - \dot{\phi}) - \frac{J_l}{Rk_h} \left[\theta_d^{(3)} + K_{v,f1}\ddot{e}_\theta + K_{p,f1}\dot{e}_\theta \right], \\ \ddot{p}_{h,d} &= -R(\ddot{\theta} - \ddot{\phi}) - \frac{J_l}{Rk_h} \left[\theta_d^{(4)} + K_{v,f1}e_\theta^{(3)} + K_{p,f1}\ddot{e}_\theta \right]. \end{aligned} \quad (8)$$

Note that we do not need to measure any second or higher order derivatives of states, since we can simply use terms from the equations of motion (5) and their derivatives. The performance of the leg angle controller during flight is shown in Fig. 7.

3.3. Body pitch control

Body pitch is controlled during stance in a similar fashion as is the leg angle during flight. To be properly synchronized with the stance time, the symmetric body pitch angle has to follow the trajectory

$$\phi_d(\eta_s) = \hat{\phi}_d \sin(\pi\rho\eta_s),$$

where the stance locomotion time η_s and the duty cycle ρ are as defined above. Note that this trajectory is derived during a ballistic flight of the system and simply specifies the body pitch trajectory during a portion of the cycle which now coincides with stance. In this case, the amplitude of the body oscillation and the leg oscillation are related as follows

$$\hat{\phi}_d = -J_b/J_l\hat{\theta}_d.$$

Since the amplitude of the leg oscillation, $\hat{\theta}_d$ has already been determined in the previous section, the desired body pitch trajectory is complete.

To track the desired body pitch trajectory, the same strategy as for the leg angle is used. However, the equations of motion during stance are different, and a simplified version we use is

$$\ddot{\phi} = Rk_h[p_h + R(\theta - \phi)] - m_b g z_{cg,b} \sin(\phi) / J_b \quad (9)$$

$$\ddot{r} = -M_{b,ul}[g \cos(\theta) + r\dot{\theta}^2] + k_l(r_0 - r + p_l) / M_{b,ul} \quad (10)$$

$$\ddot{\theta} = \left(-Rk_h[p_h + R(\theta - \phi)] - M_{bu}(r - z_{cg,bu})(2\dot{r}\dot{\theta} - r m_{b,ul} \sin\theta) \right) / [J_{l,cg} + M_{b,ul}(r - z_{cg,bu})] \quad (11)$$

where $r = p_l + q_l$ is the distance from the hip joint to toe.

The remainder of the controller development is analogous to above and is omitted here for brevity. The performance of this controller during a run is shown in Fig. 7.

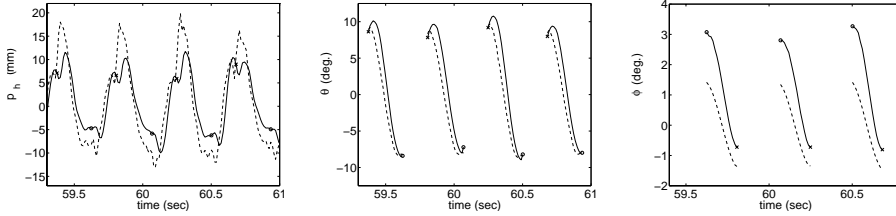


Figure 7. The performance of the hip actuator controller (left), the leg angle controller during flight (center), and the body pitch controller during stance (right) during a 1m/s run, (dash: desired, solid: actual).

4. Energetics

After having achieved stable running, as described in the previous section, we can now devote our attention to the primary motivation for the added hip compliance - the potential for energy savings. A common measure of energy expenditure is the integral of the absolute value of the instantaneous “shaft power,”

$$E_{shaft} = \int |\tau\omega| dt$$

where τ and ω are the torque and the angular velocity of the primary actuator, in our case, the leg and hip electric motors. Note that this measure does not include the motor efficiency of converting input electric power to shaft power, but does include the energy expenditure of moving the transmissions (in our case ball screws). We have summarized the energetics in Table 3 numerically, and graphically in Fig. 8, according to phases and motors. Compared to the energetics for running with a directly actuated hip [5], where the body pitch controller consumed 5J and the forward speed controller consumed 20J (at

1.2m/s), drastic reduction were achieved: The savings amount to approximately 75% for the forward speed controller and about 60% for the pitch angle controller.

	<i>Stance Phase</i>	<i>Flight Phase</i>
<i>Leg Motor</i>	Hopping Height: 12J	Leg Retraction: 10J
<i>Hip Motor</i>	Body Pitch: 2J	Forward Speed: 4J

Table 3. Energy cost of 28J per step divided by phase and actuator

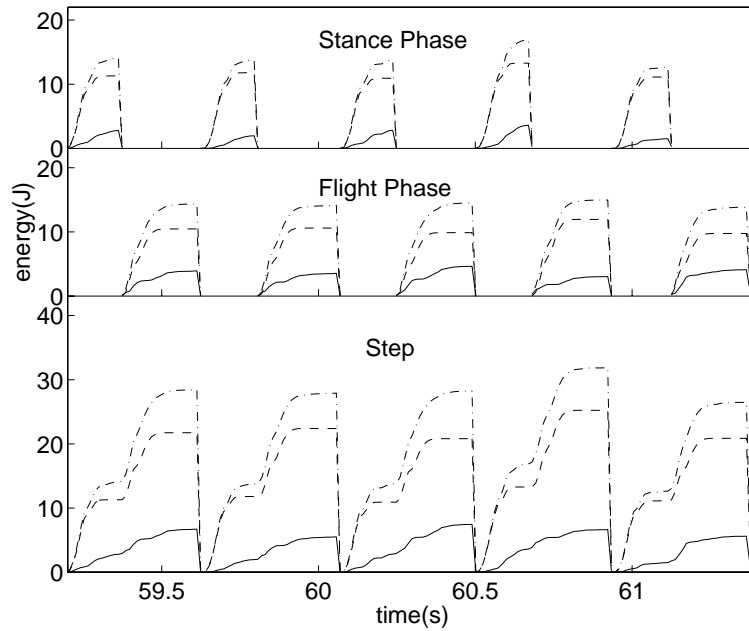


Figure 8. Experimental energetic data at 1m/s. (solid: hip motor, dashed: leg motor, dot-dash: total)

To compare this results to previous results we obtained in [5] we use the specific resistance, a standard measure of energy efficiency for mobile systems, which takes average power P , weight mg , and velocity into account,

$$\varepsilon(v) = \frac{P(v)}{mgv} = \frac{28J/hop \cdot 2.3hops/s}{18kg \cdot 9.81m/s^2 \cdot 1.0m/s} = 0.36$$

The best value reported in [5] for the ARL Monopod with directly actuated hip was $\varepsilon(1.2m/s) = 0.7$. With on board batteries and controller, ARL Monopod II is heavier (to the body and leg mass in Table 1, we have to add the mass of the moving parts of the planarizer of 1.9kg, for a total mass of 18kg), was evaluated at a slower speed (1.0m/s vs. 1.2m/s), but with 28J uses approximately half the energy, and the specific resistance, as indicated above is only $\varepsilon(1m/s) = 0.36$.

Conclusion

This paper presented the first experimental results of controlled passive dynamic running of a one legged hopping robot with leg and hip compliance. The approach is very robust to deviations from the assumptions used to derive the controller. For example, it assumes a small duty cycle (ratio of stance to flight time), which was set to $1/6$ in our previous simulations. However, in the experiments it was between $1/3$ and $1/2$, which clearly violates the straight line approximation shown in Fig. 5. In addition, the model based controllers rely on many parameters which are only approximately known. The energy savings obtained were dramatic and improved the energy efficiency of the robot by a factor of two.

References

- [1] M. Ahmadi and M. Buehler. Stable Control of a Simulated One-Legged Running Robot with Hip and Leg Compliance. *IEEE Trans. Robotics and Automation*, 13(1):96–104, Feb 1997.
- [2] R. McN. Alexander. Three Uses for Springs in Legged Locomotion. *Int. J. Robotics Research*, 9(2):53–61, 1990.
- [3] C. Francois and C. Samson. Energy Efficient Control of Running Legged Robots. A Case Study: The Planar One Legged Hopper. Technical Report 3027, Unité de recherche INRIA, Sofia-Antipolis, France, 1996.
- [4] P. Gregorio, M. Ahmadi, and M. Buehler. Experiments with an electrically actuated planar hopping robot. In T. Yoshikawa and F. Miyazaki, editors, *Experimental Robotics III*, pages 269–281. Springer-Verlag, 1994.
- [5] P. Gregorio, M. Ahmadi, and M. Buehler. Design, Control and Energetics of an Electrically Actuated Legged Robot. *IEEE Trans. Systems, Man, and Cybernetics*, 27(4):(to appear), Aug 1997.
- [6] A. Lebaudy, J. Prosser, and M. Kam. Control algorithms for a vertically-constrained one-legged hopping machine. In *Proc. IEEE Int. Conf. Decision and Control*, pages 2688–2693, 1993.
- [7] T. McGeer. Passive dynamic walking. *Int. J. Robotics Research*, 9(2):62–82, 1990.
- [8] K. V. Papantoniou. Electromechanical design for an electrically powered, actively balanced one leg planar robot. In *Proc. IEEE/RSJ Conf. Intelligent Systems and Robots*, pages 1553–1560, Osaka, Japan, 1991.
- [9] M. H. Raibert. *Legged Robots That Balance*. MIT Press, Cambridge, MA, 1986.
- [10] M. H. Raibert and C. M. Thompson. Passive dynamic running. In V. Hayward and O. Khatib, editors, *Experimental Robotics I*, pages 74–83. Springer-Verlag, NY, 1989.